mathematics

MDPI

Article

Hyperbolic Representation of the Richards Growth Model

Marcin Molski

Quantum Chemistry Department, Adam Mickiewicz University of Poznań, Uniwersytetu Poznańskiego 8, 61-614 Poznań, Poland; mamolski@amu.edu.pl; Tel.: +48-602-250-063

Abstract: The phenomenological universalities (PU) approach is employed to derive the Richards growth function in the unknown hyperbolic representation. The formula derived can be applied in theoretical modeling of sigmoid and involuted growth of biological systems. In the model proposed, the exponent in the Richards function has the following clear biological meaning: it describes the number of cells doubling, leading to an increase in a biomass of the system from m_0 (birth or hatching mass) to the limiting value m_∞ (mass at maturity). The generalized form of the universal growth function is derived. It can be employed in fitting the weight–age data for a variety of biological systems, including copepods, tumors, fish, birds, mammals and dinosaurs. Both the PU methodology and the Richards model can be effectively applied in the theoretical modeling of infectious disease outbreaks. To substantiate this assertion, the simplest PU-SIR (Susceptible–Infective–Removed) epidemiological model is considered. In this approach, it is assumed that the number of births is approximately equal to the number of deaths, while the impact of recovered (quarantined) individuals on the dynamics of the infection is negligible.

Keywords: phenomenological universalities; differential equations; sigmoidal functions; Richards model; involuted growth; infection dynamics; SIR model

MSC: 92B99; 65D10; 37N25; 34C11; 92-10

1. Introduction

Among the various mathematical models utilized in the theoretical representation of growth phenomena, the most frequently employed are the exponential, Gompertz, von Bertalanffy, West–Brown–Enquist (WBE), power law, logistic (Verhulst), and Richards (theta or generalized logistic) models [1]. These models can be systematically derived from fundamental principles [2–5] and subsequently applied to simulate changes in length, volume, weight, or cell numbers over time within complex systems. A particularly notable approach for constructing and categorizing growth models is the PU concept, introduced by Castorina, Delsanto, and Guiot (CDG) [6]. This framework enables the derivation of the exponential, Gompertz, von Bertalanffy, and WBE functions from a set of first-order differential equations, which incorporate the so-called generating function [6]

$$\Phi(x) = x + c_2x^2 + c_3x^3 + \ldots \tag{1}$$

expanded into a power series in the vicinity of $x = 0$ at the assumptions $\Phi(0) = c_0 = 0$, $c_1 = 1$. For $\Phi(x) = 0$, the CDG method generates the exponential, for $\Phi(x) = x$ the Gompertz function, whereas for $\Phi(x) = x + c_2x^2$ the von Bertalanffy and WBE functions belonging to the U_0, U_1, and U_2 classes of PU, respectively. The PU concept and CDG methodology are useful for their applicative relevance in various fields of research, including physics, chemistry, biology, ecology, engineering, economics, and social sciences [6].

check for updates

Academic Editor: Takashi Suzuki

Received: 3 March 2025
Revised: 14 April 2025
Accepted: 15 April 2025
Published: 17 April 2025

Citation: Molski, M. Hyperbolic Representation of the Richards Growth Model. *Mathematics* **2025**, *13*, 1316. https://doi.org/10.3390/math13081316

Copyright: © 2025 by the authors. Licensee MDPI, Basel, Switzerland. This article is an open access article distributed under the terms and conditions of the Creative Commons Attribution (CC BY) license (https://creativecommons.org/licenses/by/4.0/).

In particular, this strategy is extremely effective in the study of complex systems whose development is governed by nonlinear processes, resulting in the appearance of the specific growth patterns. Consequently, the CDG approach can be employed to obtain different growth models widely applied in biology, medicine, and ecology [7–9].

The PU concept has been extended [10] to include unconventional forms of the generating functions $\Phi(x) = x + c_0 + (x + c_0)^2$ and $\Phi(x) = c_1(x + c_0/c_1)^2$, applied [11] to generate the universal WBE growth curve [5] and power law (fractal) [12] function that are well known and widely applied in the fields of life sciences and beyond. Those results indicate that the form of the growth functions derived in the CDG scheme depends not only on different powers $n = 0, 1, 2 \ldots$ of the truncated series $\Phi(x)$ but also on the relationship between parameters c_0, c_1, and c_2 and the presence (absence) of the term $(x + c_0/c_1)$ in the series. Such modifications are useful in producing new forms of the growth functions known and unknown in the domain of developmental biology [1] and other sciences.

A summary of the results obtained thus far suggests that the CDG approach successfully generates all major growth functions, with the exception of the Richards function [4,13]. This observation raises two key questions: is it possible to derive the Richards function within the CDG framework, and what is the specific form of $\Phi(x)$ that yields the Richards model? The primary objective of this study is to address these questions and demonstrate that the extended PU methodology indeed generates the Richards function in a previously unrecognized hyperbolic representation. The formula derived can be applied in the theoretical modeling of sigmoid and involuted growth of biological systems. In the model proposed, the exponent in the Richards function has the following clear biological meaning: it describes the number of cells doubling, leading to an increase in a biomass of the system from birth (or hatching mass) to the limiting value, representing mass at maturity.

2. Materials and Methods

The extended CDG theory [10] is based on the set of nonlinear equations

$$\frac{d\psi(q)}{dq} - x(q)\psi(q) = 0, \qquad \frac{d\psi(q)^{\dagger}}{dq} + x(q)\psi(q)^{\dagger} = 0, \tag{2}$$

$$\frac{dx(q)}{dq} + \Phi(x) = 0, \qquad \Phi(x) = c_1(x \pm c_0/c_1) + c_2(x \pm c_0/c_1)^2 + \ldots \tag{3}$$

in which $\psi(q)$ and $\psi(q)^{\dagger}$ are growth and regression (decay) functions, respectively, whereas $\Phi(x)$ is a generating function expanded into a power series in the vicinity of $x = \pm c_0/c_1$. It significantly differs from that applied originally by [6], in particular, parameters $c_0 \neq 0$ and $c_1 \neq 1$ are taken into consideration. The set of Equations (2) and (3) produce the most important growth (regression) functions [10,11]

$$\psi(q) = \exp\left[\int_q x(q)dq + C\right] \qquad \psi(q)^{\dagger} = \exp\left[-\int_q x(q)dq + C\right] \tag{4}$$

belonging to the U_0, U_1, and U_2 classes of PU to be obtained for different powers $n = 0, 1, 2$ of the truncated series (3). One may prove that the new subclass U_2^3 of PU including the Richards growth function can be obtained by making use of the generating function

$$\Phi(x) = c_0 - c_2(x - c_0/c_1)^2 \qquad c_i > 0 \tag{5}$$

which differs from those considered so far by the presence of the minus signs and therelationship between parameters $c_i > 0$. In view of this, the solutions of the CDG Equation (2) depend not only on the order of the expansion, but also on the positive or negative values

of parameters c_i defining the system. Inserting (5) to the first of the CDG Equation (3) and integrating it with respect to x-coordinate provides

$$\int \Phi(x)^{-1} dx = -(c_0 c_2)^{-1/2} \tanh^{-1}\left[\frac{c_2(c_0 - c_1 x)}{c_1\sqrt{c_0 c_2}}\right] = -q, \tag{6}$$

which can be reverted to the form

$$x(q) = -\sqrt{\frac{c_0}{c_2}} \tanh(q\sqrt{c_0 c_2}) + \frac{c_0}{c_1}. \tag{7}$$

Taking advantage of Equations (4) and (7), one may derive $\psi(q)$ as follows:

$$\psi(q) = \psi_0 \exp\left(\frac{c_0}{c_1} q\right)\left[\tanh^2(q\sqrt{c_0 c_2}) - 1\right]^{\frac{1}{2c_2}} \tag{8}$$

or alternatively, by using the identity $\cosh^{-2}(z) = 1 - \tanh^2(z)$, as follows:

$$\psi(q) = \psi_0 i^{1/c_2} \exp\left(\frac{c_0}{c_1} q\right) \cosh(q\sqrt{c_0 c_2})^{-\frac{1}{c_2}}. \tag{9}$$

Here, $i = \sqrt{-1}$ is an imaginary number. By taking advantage of the relationship $\cosh(z) = [\exp(z) + \exp(-z)]/2$, function (9) can be rewritten to the exponential form

$$\psi(q) = \psi_0 (2i)^{\frac{1}{c_2}} \exp\left[\left(\frac{c_0}{c_1} - \sqrt{\frac{c_0}{c_2}}\right) q\right][1 + \exp(-2q\sqrt{c_0 c_2})]^{-\frac{1}{c_2}}, \tag{10}$$

which can be treated as a template for generating different growth models for the function (5). For example, the classes of sigmoid, involuted or exponential solutions can be obtained for

$$\frac{c_0}{c_1} - \sqrt{\frac{c_0}{c_2}} \begin{cases} = 0 & \text{Sigmoid} \\ < 0 & \text{Involuted} \\ > 0 & \text{Exponential} \end{cases} \tag{11}$$

The sigmoid version of function (10) has an inflection point q_i and takes the value $\psi(q_i)$ equal to

$$q_i = -\frac{\ln(c_2)}{2\sqrt{c_0 c_2}}, \qquad \psi(q_i) = \psi_0 (2i)^{\frac{1}{c_2}} (1 + c_2)^{-\frac{1}{c_2}}. \tag{12}$$

The Richards growth model in the original form $\psi(q) = \Theta(t)$ is recovered by redefining the parameters c_i in function (10):

$$\{c_0, c_1, c_2\} \longrightarrow \{b', c'\}, \qquad \frac{c_0}{c_1} - \sqrt{\frac{c_0}{c_2}} = 0 \tag{13}$$

$$2\sqrt{c_0 c_2} = 2c_1 = b'c', \quad c_2 = b', \quad q = t - t_i' + \ln(b')/b'c' \tag{14}$$

resulting in the conversion of Equation (10) to the form

$$\Theta(t) = \Theta_\infty\left\{1 + b' \exp\left[-b'c'(t - t_i')\right]\right\}^{-1/b'}. \tag{15}$$

It represents the Richards function in which $\Theta_\infty = \psi_0 (2i)^{1/b'}$ stands for the limiting value of $\Theta(t \to \infty) = \Theta_\infty$, whereas t_i' is an inflection point satisfying $(d^2\Theta(t)/dt^2)_{t=t_i'} = 0$. Taking into account the initial condition $\Theta(t \to 0) = \Theta_0$, Equation (15) can be changed to the form

$$\Theta(t) = \Theta_0\left[1 + b' \exp\left(b'c't_i'\right)\right]^{1/b'}\left\{1 + b' \exp\left[-b'c'(t - t_i')\right]\right\}^{-1/b'}, \tag{16}$$

which is useful in the fitting of experimental data when Θ_0, instead of Θ_∞, is determined.

In this work, we propose to use an alternative parametrization

$$\{c_0, c_1, c_2\} \longrightarrow \{a, b, c\} \tag{17}$$

$$c_0 = bc^2, \quad c_1 = \frac{bc}{a}, \quad c_2 = \frac{1}{b}, \quad \sqrt{c_0 c_2} = c, \quad q = t - t_0 \tag{18}$$

converting functions (9) and (10) to the equivalent hyperbolic and exponential forms

$$\psi(t) = \psi_0 i^b \exp[ac(t - t_0)] \cosh[c(t - t_0)]^{-b}, \tag{19}$$

$$\psi(t) = \psi_0 (2i)^b \exp[(a - b)c(t - t_0)]\{1 + \exp[-2c(t - t_0)]\}^{-b}. \tag{20}$$

To validate and demonstrate the practical utility of the derived formulae, they were applied to determine the parameters of the Richards model, which characterizes sigmoidal growth (e.g., copepods, tumors, fish, birds, mammals, dinosaurs) and involuted growth (e.g., thymus in mammals or bursa of Fabricius in birds) in biological systems. The parameters were estimated by fitting the various experimental datasets using a nonlinear least-squares routine, with statistical weights assigned as the inverse squares of the standard deviations (SDs) associated with the data [14]. In cases where SDs were unavailable, the data were weighted by the reciprocal mass of the system. This approach was originally developed and applied by Laird [15] in the fitting of tumor growth data. For computational analysis, an executable Fortran-based program designed for numerical data analysis was utilized [14]. This program enables the estimation of freely fitted parameters alongside their associated standard errors, as well as the assessment of multiple indicators of the goodness of fit. Specifically, the following indicators were considered:

(i) The normalized standard deviation (*NSD*):

$$NSD = \sqrt{\frac{1}{N_D - N_P} \sum_{i=1}^{N_D} \left(\frac{m_i^{exp} - m_i^{theo}}{u_i} \right)^2} \tag{21}$$

in which N_D and N_P denote the numbers of data and parameters fitted, u_i is the *SD* of i-th experimental mass m_i^{exp}, whereas m_i^{theo} is the theoretically calculated mass by the model function. If reproduction of the data is performed within u_i, then $NSD \approx 1$, and the theory reproduces the data with experimental accuracy.

(ii) The coefficient of determination R^2:

$$R^2 = 1 - \frac{\sum_{i=1}^{N_D} \left(m_i^{exp} - m_i^{theo} \right)^2}{\sum_{i=1}^{N_D} \left(m_i^{exp} - \frac{1}{N_D} \sum_{i=1}^{N_D} m_i^{theo} \right)^2} \tag{22}$$

where the best fits are represented by $R^2 \approx 1$.

(iii) The standard deviation (*SD*):

$$SD = \sqrt{\frac{\sum_{i=1}^{N_D} \left(m_i^{exp} - m_i^{theo} \right)^2}{N_D}} \tag{23}$$

applied together with R^2 when the experimental SDs of the data are unavailable.

(iv) Akaike Information Criterion (AIC) and Bayesian Information Criterion (BIC) defined in [16] and [17], respectively: They have been used to select the best model with the optimal number of parameters fitted and to avoid overfitting. The smaller values of

AIC and BIC indicate the model more preferred and statistically reliable. The explicit form of the AIC and BIC formulae used in the calculations is presented in [14].

The results presented in Tables 1 and 2 can also be reproduced using other relevant software employed for fitting age–weight data. For example, calculations conducted with SigmaPlot version 11 yielded values that were either identical to or consistent with those reported in Tables 1 and 2, within the estimated error range. However, an exception was identified in which SigmaPlot was unable to fit the parameter m_0 for the *Tyrannosaurus rex* data, whereas the Fortran program successfully generated this parameter. In this case, m_0 should be constrained to the value of 2.06 [kg], as estimated by Myhrvold [18]. Calculations performed in the constrained scheme provided $b = 11.71(11)$ [y^{-1}] and $c = 0.0766(37)$, which are in full agreement with the results presented in Table 1.

Table 1. The parameters of the hyperbolic Richards function (40) obtained by the fit of N_D experimental weight–age data points. The uncertainty in parentheses is one estimated standard deviation in units of the last quoted digits of the values of parameters fitted.

Parameter	*C. pacificus*	FJ Cancer	*T. Rex*
m_0	4.83(80) [g × 10^{-6}]	0.0199(116) [g]	2.04(87) [Kg]
c [d^{-1}]	0.0873(65)	0.0303(35)	0.0747(48) [y^{-1}]
b	6.20(18)	10.99(64)	11.77(61)
SD	4.568 [g × 10^{-6}]	0.438 [g]	283 [Kg]
R^2	0.996	0.995	0.979
N_D	8	7	8
	Chicken	**Zebra**	**Tilapia**
m_0 [g]	35.5(1.1)	33,864(1858)	5.83(44)
c [d^{-1}]	0.0155(4)	0.0024(2)	0.0089(5)
b	5.953(61)	3.22(81)	5.93(12)
NSD	0.600	0.669	0.611
R^2	0.993	0.950	0.951
N_D	28	17	13

Table 2. The parameters of the involuted Richards functions (35) and (37) obtained by the fit of 12 experimental relative weight–age data points in units [g/100 g] [19] for the thymi of male Wistar rats and 12 data representing absolute weights [mg] of bursa of Fabricius in Chinese yellow quail [20]. The uncertainty in parentheses is one estimated standard deviation in units of the last quoted digits of the values of the parameters fitted.

	Thymus		Bursa of Fabricius	
Parameter	**Equation (35)**	**Equation (37)**	**Equation (35)**	**Equation (37)**
m_0	0.103(11)	0.106(11)	4.60(3.90)	9.01(2.01)
a	2.24(16)	2.44(28)	4.86(1.25)	7.16(1.89)
b	2.42(16)	2.65(30)	5.12(1.22)	7.69(1.86)
c [d^{-1}]	0.086(12)	0.083(11)	0.0613(193)	0.0501(99)
d = b − a	0.182(35)	0.210(50)	0.26(10)	0.53(17)
f	0	0.017(16)	0	7.58(1.54)
NSD	1.0684	1.0707	2.1895	1.3924
R^2	0.9860	0.9877	0.9453	0.9815
AIC	−94	−91	58	50
BIC	−96	−95	56	46

3. Results

Taking into account the relation (11), one may consider two classes of solutions produced by (19) and (20): sigmoid for $a = b$ and involuted for $a < b$, which will be analyzed separately in the next subsections.

3.1. Sigmoid Richards Growth

To obtain a sigmoid version ($a = b$) of the Richards functions (19) and (20) that are useful in the fitting of experimental data, especially weight–age data $\psi(t) = m(t)$, let us consider their limit values:

$$m(t \to 0) = \psi_0 i^b \exp[-bct_0] \cosh[-ct_0]^{-b} = m_0, \tag{24}$$

$$m(t \to 0) = \psi_0 (2i)^b \{1 + \exp[2ct_0]\}^{-b} = m_0 \tag{25}$$

in which m_0 is an initial value of the Richards function. Having derived the equations specified above, one may rewrite (19) and (20) to the equivalent forms

$$m(t) = m_0 \frac{\exp[bc(t - t_0)] \cosh[c(t - t_0)]^{-b}}{\exp[-bct_0] \cosh[-ct_0]^{-b}}, \tag{26}$$

$$m(t) = m_0 \frac{\{1 + \exp[-2c(t - t_0)]\}^{-b}}{[1 + \exp(2ct_0)]^{-b}}. \tag{27}$$

Now, let us consider the asymptotic limit of (27)

$$m(t \to \infty) = m_0 [1 + \exp(2ct_0)]^b = m_\infty, \tag{28}$$

which, for $t_0 = 0$, reduces to a simple formula

$$m(t \to \infty) = m_0 2^b = m_\infty, \tag{29}$$

which allows for a precise biological interpretation of the b-parameter for growing biosystems: it describes the number of cells doubling, leading to an increase in a biomass from m_0 (in the case of animals, it is birth or hatching mass) to the limiting value m_∞ (mass at maturity). The interpretation proposed is correct for $t_0 = 0$ and predicts that the value of b-parameter should be equal (within standard error) to an integer number. The results of the test calculations presented in Table 1 confirm this hypothesis.

Finally, one may pass to generate the equation governing the Richards sigmoid growth, by substituting Equations (18) into (7) and then Equations (7) into (2), yielding

$$\left\{ \frac{d}{dt} + cb \tanh[c(t - t_0)] - cb \right\} m(t) = 0, \tag{30}$$

or alternatively

$$\frac{1}{m(t)} \frac{dm(t)}{dt} = 2bc \left[1 - \left(\frac{m(t)}{m_\infty} \right)^{1/b} \right]. \tag{31}$$

For comparison, the original Richards growth function (20) satisfies

$$\frac{1}{\Theta(t)} \frac{d\Theta(t)}{dt} = c' \left[1 - \left(\frac{\Theta(t)}{\Theta_\infty} \right)^{b'} \right]; \tag{32}$$

consequently, both models are equivalent, and characterized by the growth rates $2c$ and c', respectively. In this way, we have complete characteristics of the dynamics of the sigmoid Richards growth characterized by the hyperbolic function (26) or its alternative exponential version (27).

To demonstrate the applicability of the functions (26) and (27) in the quantitative analysis of the weight–age data and to prove the correctness of the relation (29), we employ them to model the post-natal growth of fish, tilapia nile *Oreochromis niloticus* [21]; bird,

Athens-Canadian male chicken *Gallus gallus domesticus* [22]; and mammal, zebra *Equus Burchelli antiquorum* [23], that were already tested in our previous work [14] using the von Bertalanffy growth function [2,3]. We verified that the inclusion of only post-natal data allows for their satisfactory reproduction with a fixed value of the parameter $t_0 = 0$. These data were supplemented with additional ones obtained for submillimeter multicellular marine copepod (metazoan) *Calanus pacificus* [24], Flexner–Jobling (FJ) cancer [25], and dinosaur *Tyrannosaurus rex* [18]. In the last case, the Myhrvold data were enriched by hatchling mass $m_0 = 2.06(13)$ [Kg] reported by [26]. The results of calculations are presented in Table 1.

3.2. Involuted Richards Growth

Now, let us focus our attention to the general expressions (19) and (20) with $\psi(t) = M(t)$ and $M(t = 0) = m_0$ for $a < b$

$$M(t) = m_0 \frac{\exp[ac(t - t_0)] \cosh[c(t - t_0)]^{-b}}{\exp(-act_0) \cosh(-ct_0)^{-b}}, \tag{33}$$

$$M(t) = m_0 \frac{\exp[(a - b)ct)]\{1 + \exp[-2c(t - t_0)]\}^{-b}}{[1 + \exp(2ct_0)]^{-b}}. \tag{34}$$

They represent a family of curves whose shape depends on the value of a-parameter in relation to b. For $a = b$, one always obtains the sigmoid Richards curve, whereas for $a < b$, formulae (33) and (34) describe the systems which undergo involution in the course of time (e.g., thymus in mammals or bursa of Fabricius in birds). The plots of function (34) for different values of a in relation to fixed b are presented in Figure 1. Its analysis reveals that the shape of the involuted Richards curves depends on the difference $d = b - a$ between parameters defining the model. Consequently, one may rewrite (33) in the form of an involuted Richards function $m(t)$:

$$M(t) = \exp[(a - b)ct]m(t), \qquad a < b \tag{35}$$

in which $M(t) \to m(t)$ for $b \to a$ stands for the sigmoidal Richards growth model (27). The function (35) satisfies the kinetic equation of the involuted growth:

$$\left\{ \frac{d}{dt} + cb \tanh[c(t - t_0)] - ca \right\} M(t) = 0 \tag{36}$$

as it is a generalized form of the expression (30).

Because $\lim_{t\to\infty} M(t) = 0$, hence, in the analysis of the data for the systems with asymptotic behavior $\lim_{t\to\infty} M(t) = f$, the modified function (35)

$$M(t) = \exp[(a - b)ct]m(t) + f \tag{37}$$

should be taken into consideration. In such circumstances, the initial value of $M(t)$ is defined as follows:

$$M_0 = \lim_{t\to 0} M(t) = m_0 + f. \tag{38}$$

Consequently, the functions (33) and (34) should be changed to the forms

$$M(t) = (M_0 - f) \frac{\exp(act) \cosh[c(t - t_0)]^{-b}}{\cosh(-ct_0)^{-b}} + f, \tag{39}$$

$$M(t) = (M_0 - f)\frac{\exp[(a-b)ct]\{1+\exp[-2c(t-t_0)]\}^{-b}}{\exp[1+\exp(2ct_0)]^{-b}} + f. \quad (40)$$

It should be pointed out that the limit $M(t \to \infty) = f$ has only mathematical meaning due to the restricted existence time of biological systems; hence, both functions (35) and (37) should describe an involuted growth in shorter intervals with comparable accuracy. In order to verify this thesis and demonstrate the usefulness of functions (39) and (40) in the analysis of the involuted growth, we fitted 12 data points representing thymic-to-body mass ratio of male Wistar rats reported in [19]. They were measured in the interval (0–240) [d] and $SD = 0.014$ [mg/100 g]. Application of the relative instead of absolute thymus weights guarantees the existence of an asymptote with $f \neq 0$, while the fit of the absolute weight data provides the unsatisfactory value $f = -0.0033 \pm 0.0135$. The results of calculations are presented in Tables 2 and 3, whereas plots of functions (36) and (37) are displayed in Figure 2.

In the second analysis of the involuted growth, we fitted 12 experimental data points representing the absolute weights of bursa of Fabricius in Chinese yellow quail measured by [20] in the interval (0–252) [d] with variable accuracy SD = 1.21–7.71 [mg]. The results of calculations are presented in Tables 2 and 4, whereas the plots of functions (36) and (37) are displayed in Figure 3.

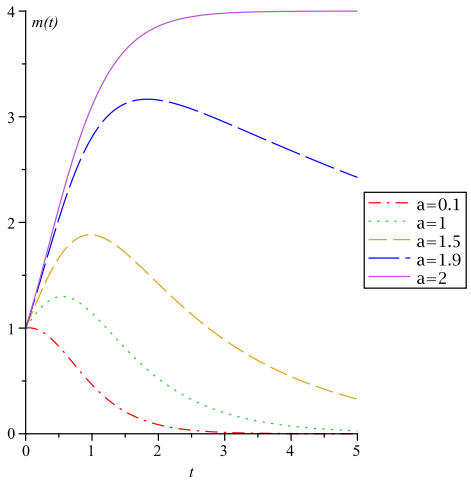


Figure 1. The plots of the function (34) for different values of a and $b = 2$, $c = m_0 = 1$, and $t_0 = 0$. For $a = b = 2$, one obtains the sigmoid Richards growth function.

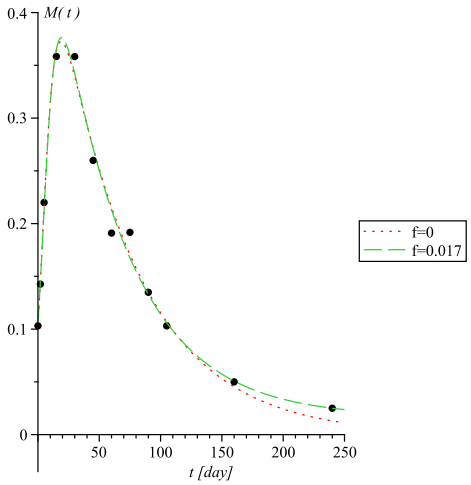


Figure 2. The plots of involuted Richards functions (35) and (37) defined by parameters from Table 2. Black circles represent the thymic-to-body mass ratio of male Wistar rats measured by [19].

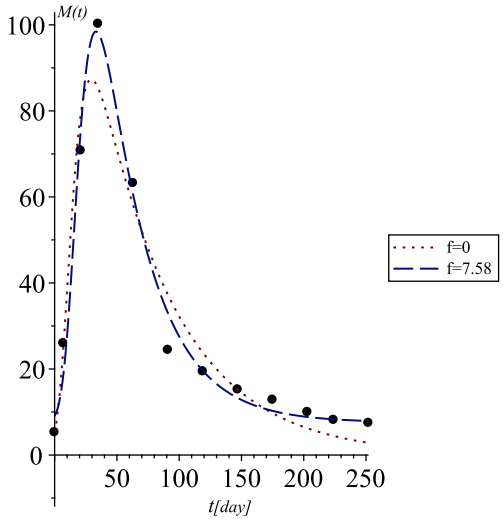


Figure 3. The plots of involuted Richards functions (35) and (37) defined by parameters from Table 2. Black circles represent the absolute weights of bursa of Fabricius yellow quail measured by [20].

Table 3. Theoretical reproduction of 12 experimental relative weight–age data measured with $SD = u_i = 0.0140$ [g/100 g] by [19] for thymi of male Wistar rats by the involuted Richards functions (35) and (37) with parameters from Table 2.

		f = 0		**f = 0.017(16)**	
Time [d]	$m_i^{exp}(u_i)$	$\frac{m_i^{exp}-m_i^{theo}}{u_i}$	m_i^{theo}	$\frac{m_i^{exp}-m_i^{theo}}{u_i}$	m_i^{theo}
0	0.1031	0.0264	0.1027	−0.1746	0.1055
2	0.1426	−0.2036	0.1455	−0.1913	0.1453
5	0.2200	0.2981	0.2158	0.5025	0.2130
15	0.3584	−0.3778	0.3637	−0.4991	0.3654
30	0.3583	1.3569	0.3393	1.1510	0.3422
45	0.2599	−0.8691	0.2721	−0.8170	0.2713
60	0.1910	−1.7526	0.2155	−1.5633	0.2129
75	0.1917	1.5076	0.1706	1.7176	0.1677
90	0.1349	−0.0080	0.1350	0.1476	0.1328
105	0.1031	−0.2679	0.1069	−0.2100	0.1060
160	0.0500	0.3344	0.0453	−0.0587	0.0508
240	0.0250	0.8561	0.0130	−0.0047	0.0251

Table 4. Theoretical reproduction of 12 experimental data measured with $SD = u_i$ for absolute weights ([mg]) of bursa of Fabricius in Chinese yellow quail [20] by the involuted Richards functions (35) and (37) with parameters from Table 2.

		f = 0		**f = 7.58(1.54)**	
Time [d]	$m_i^{exp}(u_i)$	$\frac{m_i^{exp}-m_i^{theo}}{u_i}$	m_i^{theo}	$\frac{m_i^{exp}-m_i^{theo}}{u_i}$	m_i^{theo}
0	5.28(2.15)	0.3143	4.6041	−1.7372	9.0148
7	25.97(4.92)	0.3915	24.0437	1.5245	18.4694
21	70.77(7.71)	−1.1872	79.9236	−0.6558	75.8266
35	100.23(6.47)	2.2507	85.6682	0.3164	98.1829
63	63.21(3.90)	1.2845	58.2003	0.6778	60.5664
91	24.43(3.88)	−3.2998	37.2332	−2.1928	32.9379
119	19.43(1.96)	−2.2175	23.7763	−0.0738	19.5746
147	15.23(1.75)	0.0273	15.1822	1.1271	13.2599
175	12.83(2.54)	1.2345	9.6944	1.0092	10.2576
203	9.98(3.52)	1.0766	6.1903	0.3159	8.8678
224	8.15(1.21)	3.0811	4.4218	−0.1455	8.3261
252	7.45(3.28)	1.4105	2.8235	−0.1517	7.9477

3.3. Generalized Universal Growth Curve

The Richards function (27) can be converted to the form

$$R(y) = \frac{1}{1+\exp(-y)}, \tag{41}$$

defined by the dimensionless time y and mass $R(y)$

$$y = 2c(t - t_0), \qquad R(y) = \left\{ \frac{m(t)}{m_0[1+\exp(2ct_0)]^b} \right\}^{1/b}, \tag{42}$$

which, for $t_0 = 0$, reduces to

$$y = 2ct, \qquad R(y) = \left[\frac{m(t)}{m_0 2^b} \right]^{1/b}. \tag{43}$$

Equation (41) is a generalization of the universal growth function $R(y) = 1 - \exp(-y)$ introduced by [5]. The last thesis can be proven by employing the approximation $R(y) = 1/([1+\exp(-y)] \approx 1 - \exp(-y)$. The generalized universal growth curve (41) and experimental weight–age data points expressed in terms of y and $R(y)$ are presented in Figure 4. Its analysis reveals that all the data considered satisfy a universal law of growth (41), which can be successfully employed in fitting the weight–age data for a variety of biological systems, including copepods, tumors, fish, birds, mammals, and dinosaurs, ranging from metazoan *Calanus pacificus* with $m_\infty = 5.8 \times 10^{-3}$ [g] and ending on *Tyrannosaurus rex* with $m_\infty = 7.124 \times 10^6$ [g] (the values of m_∞ were calculated from Equation (29) and parameters from Table 1. It is noteworthy that the latter value conforms acceptably with $m_\infty = 7.000(980) \times 10^6$ [g], as reported by Lee [26].

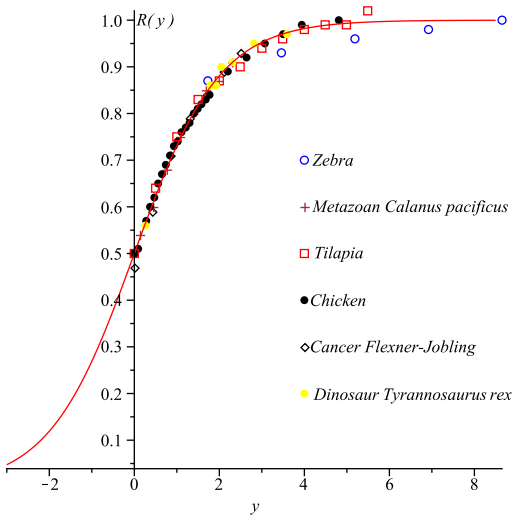


Figure 4. The generalized universal growth curve (41) and experimental data points for exemplary biological systems taken into consideration.

3.4. PU-SIR Epidemic Model

The PU methodology can be successfully applied in modeling the systems whose time evolution depends on several coupled processes. As an example, the use in the description of ecological population growth can be given [9]. This approach can be adapted to the prediction of the outbreak of infective diseases. To substantiate this thesis, we will use the SIR epidemiological model [27–30] in a simplified form, as proposed by [31]. In this approach, the number of births is approximately equal to the number of deaths, and,

additionally, it is assumed that the individuals in the infected class restrict its social activity after being recovered (quarantined). Consequently, the impact of recovered individuals on the dynamics of the infection is negligible, and the denominator in the transmission term in the original SIR model is the sum of susceptible and infected individuals $S + I$ and not the total population $N = S + I + R$, including recovered class R. In view of this, the simplified SIR approach is based on the following set of equations [31]:

$$\frac{dS(q)}{dq} = -\beta\left[\frac{I(q)}{S(q)+I(q)}\right]S(q), \quad \frac{dI(q)}{dq} = \beta\left[\frac{S(q)}{S(q)+I(q)} - \gamma\right]I(q), \tag{44}$$

$$\frac{dR(q)}{dq} = \gamma\left[\frac{I(q)}{R(q)}\right]R(q), \quad S(q) + I(q) + R(q) = N, \tag{45}$$

in which $S(q)$, $I(q)$, and $R(q)$ represent the numbers of individuals in the susceptible, infective, and removed (recovered, quarantined) classes at the time q; β and γ are the transmission and recovery rates, whereas N stands for the total (constant) population. Taking into account the relation (45), we only have to solve the set of Equation (44) and then $R(q)$ can be determined from (45). Equation (44) can be rewritten according to the PU convention in the following manner:

$$\frac{dS}{dq} = x(q)S, \quad \frac{dI}{dq} = y(q)I, \tag{46}$$

$$x(q) = -\beta\left[\frac{I}{S+I}\right], \quad y(q) = \beta\left[\frac{S}{S+I}\right] - \gamma, \tag{47}$$

or, alternatively, in a compact matrix notation:

$$\begin{bmatrix} x, & x+\beta \\ y+\gamma-\beta, & y+\gamma \end{bmatrix}\begin{bmatrix} S \\ I \end{bmatrix} = 0. \tag{48}$$

Here, we use the normalized forms of $S(q)$ and $I(q)$:

$$S = \frac{S(q)}{S(0)}, \quad \lim_{q\to 0} S = 1, \quad I = \frac{I(q)}{I(0)} \quad \lim_{q\to 0} I = 1, \tag{49}$$

in which $S(0)$ denotes the initial number of individuals in the susceptible class who will eventually be infected, while $I(0)$ stands for an initial number of infections. Since $R(0) = 0$, the term *normalized function* R means that it is defined by the equation $R = N - S - I$ containing the normalized functions S and I.

Employing Equations (47) and (49), one may determine the initial values of $x(q)$ and $y(q)$:

$$\lim_{q\to 0} x(q) = -\frac{\beta}{2}, \qquad \lim_{q\to 0} y(q) = \frac{\beta}{2} - \gamma \tag{50}$$

The above expressions and $q = (0, t)$ are useful in calculating definite integrals. The set of homogenous Equation (48) has non-trivial solutions provided that the determinant of the squared matrix is equal to zero, resulting in the relationships

$$x(q) - [y(q) - \gamma + \beta] = 0, \quad I = -\frac{x}{\beta + x}S. \tag{51}$$

Differentiating the first of the above equations with respect to the temporal q-coordinate and taking into account the relation (3) adapted to the two-component PU model

$$\frac{dx(q)}{dq} + \frac{d[-y(q) - \gamma + \beta]}{dq} = -\Phi(x) + \Phi(y) = 0, \tag{52}$$

one obtains the important information that in the PU-SIR scheme, only $\Phi(x)$ and $x(q)$ or $\Phi(y)$ and $y(q)$ are required to obtain the final solutions:

$$S = \exp\left[-\int_0^t x(q)dq\right] \tag{53}$$

and

$$I = \exp\left[\int_0^t y(q)dq\right] = S\exp[(\beta - \gamma)t], \tag{54}$$

in which the relation (51) is taken into account. A comparison of Equations (51) and (54) provides the relationship

$$\exp[(\beta - \gamma)t] = -\frac{x}{x + \beta}, \tag{55}$$

and important formulae

$$x(t) = -\frac{\beta\exp[(\beta - \gamma)t]}{\exp[(\beta - \gamma)t] + 1}, \quad t(x) = \ln\left[-\left(\frac{x}{\beta + x}\right)^{\frac{1}{\beta - \gamma}}\right]. \tag{56}$$

The former permits calculating S and I by taking advantage of Equations (53) and (54):

$$S = 2^{\frac{\beta}{\beta - \gamma}}\{1 + \exp[(\beta - \gamma)t]\}^{-\frac{\beta}{\beta - \gamma}} \tag{57}$$

$$I = 2^{\frac{\beta}{\beta - \gamma}}\{1 + \exp[(\beta - \gamma)t]\}^{-\frac{\beta}{\beta - \gamma}}\exp[(\beta - \gamma)t], \tag{58}$$

while the latter yields the implicit formula for the generating function $\Phi(x)$ by making use of the relation (3) in a slightly modified version:

$$\Phi(x) = -\left[\frac{dt(x)}{dx}\right]^{-1} = -\beta^{-1}(\beta - \gamma)(\beta + x)x. \tag{59}$$

One may rewrite $\Phi(x)$ specified above into the form consistent with Equation (5):

$$\Phi(x) = \frac{(\beta - \gamma)\beta}{4} - \frac{(\beta - \gamma)}{\beta}\left(x + \frac{\beta}{2}\right)^2 = c_0 - c_2\left(x + \frac{c_0}{c_1}\right)^2, \tag{60}$$

whereas Equations (57) and (58) can be given in the hyperbolic representation:

$$S = \exp\left(-\frac{\beta}{2}t\right)\cosh\left[\frac{(\beta - \gamma)}{2}t\right]^{-\frac{\beta}{\beta - \gamma}}, \tag{61}$$

$$I = \exp\left(-\frac{\beta}{2}t\right)\cosh\left[\frac{(\beta - \gamma)}{2}t\right]^{-\frac{\beta}{\beta - \gamma}}\exp[(\beta - \gamma)t]. \tag{62}$$

Additionally, from (45), we have

$$R = N - S - I = N - S\{1 + \exp[(\beta - \gamma)t]\}, \quad \frac{dR}{dt} = \gamma I, \tag{63}$$

which are valid for exponential (57) and hyperbolic (61) representations of S. Plots of the S, I, and R functions for the selected values of β and γ are presented in Figure 5. Equation (60) reveals that the generating function in the PU-SIR model differs from (5) by the sign in the second-order term. Consequently, all formulae derived for $\Phi(x)$ in the form (5) can

be converted to those appearing in the PU-SIR model by the substitution $c_1 \to -c_1$ and $\sqrt{c_0 c_2} \to -\sqrt{c_0 c_2}$ in the original equations. In particular, the general solution (10) for the generating function (60) takes the form

$$\psi(q) = \psi_0 (2i)^{\frac{1}{c_2}} \exp\left[\left(-\frac{c_0}{c_1} + \sqrt{\frac{c_0}{c_2}}\right) q\right] [1 + \exp(2q\sqrt{c_0 c_2})]^{-\frac{1}{c_2}}. \tag{64}$$

The transmission and recovery rates β and γ in the SIR model proposed by [31] enable the calculation of the basic reproductive ratio $R_0 = \beta/\gamma$. This descriptor is extremely useful in guiding the control strategies for epidemics. According to the epidemiological definition [32], it describes the average number of secondary cases produced by one infected individual introduced into a population of susceptible individuals.

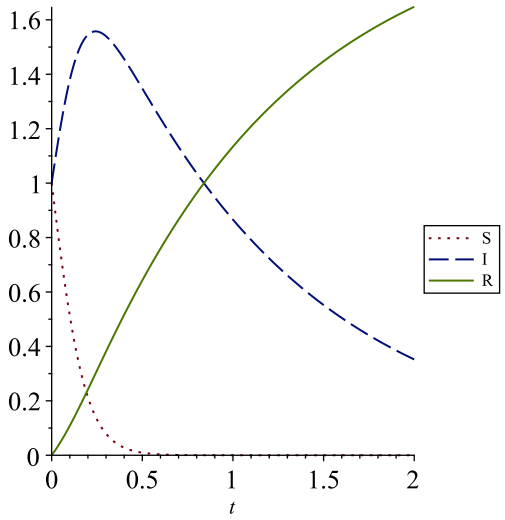


Figure 5. The plots of normalized S, I, and R functions for $\beta = 10.8$, $\gamma = 0.9$, and $S + I + R = 2$.

4. Discussion

The original Richards function is of empirical nature that characterizes many incredible coincidences with biological, medical, ecological, and epidemic data, despite the fact that it depends on the b-exponent that does not have a clear biological meaning [31]. In the SIR model proposed by [31], the exponent in the Richards function $b = 1/(1 - R_0^{-1})$ has a one-to-one nonlinear correspondence to the basic reproduction number R_0 (or reproductive ratio). In this work, we propose another interpretation of b-parameter; it describes the number of cells doubling, leading to an increase in a biomass of the system from m_0 (birth or hatching mass) to the limiting value m_∞ (mass at maturity). This interpretation is valid for sigmoidal but can also be extended to involuted growth. Since the involuted Richards Formula (35) is the product of decay $\exp[(a-b)ct]$ and sigmoidal $m(t)$ functions, b-exponent characterizes the pattern formation of the organ at the hypothetical absence of involution represented by the a-dependent decay term. This interpretation becomes clear if the limit

$$\lim_{t\to\infty} \exp[(a-b)ct] m(t) = 0 \cdot m_0 2^b = 0 \cdot m_\infty, \qquad t_0 = 0 \tag{65}$$

will be taken into consideration. A look into Table 1 reveals that the b-parameter fitted to the biological data considered is equal (or close) to the integer in the range of the standard deviations quoted. The calculations provided the following b-values: 6.20(18), 10.99(64),

5.93(12), 5.953(61), 3.22(81), and 11.77(61). One may confront them with the values generated from (29), specified in an alternative form:

$$b = \frac{1}{\ln(2)} \ln\left(\frac{m_\infty}{m_0}\right) \tag{66}$$

with m_∞ and m_0 measured or fitted by other models of growth. For example, in the case of *T. rex*, $m_\infty = 7000(980)$ [Kg] and $m_0 = 2.06(13)$ [Kg] are estimated by the von Bertalanffy model [26], yielding $b = 11.73$; for the FJ cancer, $m_\infty = 48.4$ [g] and $m_0 = 0.015$ [g] are calculated using the Gompertz function [15], providing $b = 11.66$; for Athens-Canadian male chicken, $m_\infty = 2192.7$ [g] and $m_0 = 37.00(3.02)$ [g] are determined by the logistic model [22], supplying $b = 5.889$; for zebra, $m_\infty = 316.86(2.10)$ [Kg] and $m_0 = 33.70(2.78)$ [g] are obtained from the von Bertalanffy model [23], giving $b = 3.23$. All b-values calculated in this way conform acceptably with those presented in Table 1.

The b-interpretation proposed is no longer substantiated in the case of relative thymic-to-body mass ratio data for male Wistar rats reproduced by the function (37) with $f = 0$ and $b = 2.42(16)$. The situation changes radically when b is determined using the absolute thymus weight–age data [19]. The calculations performed with $f = 0$ provided the parameters $a = 5.88(30)$, $b = 5.96(58)$, $c = 0.0410(41)$ [d^{-1}], and $m_0 = 0.0060(25)$ [g], fitted with $NSD = 1.608$ and $R^2 = 0.976$, clearly indicating that b-exponent for this organ is again represented by an integer number. We conclude that the interpretation proposed is valid only for absolute mass of organisms and organs but fails in the case of abstractive relative mass of the system.

A look into Tables 2 and 3 reveals that both functions (36) and (37) describe an involuted thymus growth in a short time interval $t \in$ (1–160) [d] with identical accuracy. A discrepancy appears only for $M(t = 240\ [d])$ [g], indicating that the data collected for a larger time period should be analyzed only by means of function (37) with $f \neq 0$. In this way, the proper asymptotic behavior of the involuted Richards function will be taken into consideration. However, the values of the AIC and BIC indicators reported in Table 2 clearly inform us that in the case of reproducing the data for rat thymus, the inclusion of the f-parameter leads to the deterioration of the statistical characteristics of the fit, unlike in the case of data for the bursa of Fabricius. It can be observed that the AIC and BIC goodness-of-fit metrics provide guidance on the selection of the number of parameters that yield a statistically optimal fit to the experimental data. In this manner, the issue of overfitting can be identified and mitigated.

5. Conclusions

The findings of this study confirm that the PU methodology is highly effective in generating growth functions, with potential applications across various fields of the life sciences. In particular, this approach can be employed to obtain analytical solutions to the differential equations of the SIR model, thereby expanding the range of existing methods utilized for this purpose [33–36]. Furthermore, the application of a modified form of the generating function (5) enables the derivation of the sigmoidal and involuted Richards function in a previously unrecognized hyperbolic representation. This formulation extends the broad class of re-parameterized and unified Richards models discussed by [13], incorporating a novel variant of this widely utilized function. The derived formula has practical applications in epidemic modeling and the quantitative analysis of growth in biological systems, including thymus, bursa of Fabricius, copepods, tumors, fish, birds, mammals, and even dinosaurs. Additionally, it has been demonstrated that the analyzed growth data conform to a universal growth curve (41), which generalizes the function traditionally used for fitting weight–age data across a diverse range of species [5]. The

approach proposed facilitates a precise biological interpretation of the b-exponent in the Richards functions (19) and (20). Specifically, the interpretation describes the number of cell doublings that contribute to the increase in biomass, from the birth or hatching mass to the limiting value representing the mass at maturity. The proposed interpretation predicts that the bb-parameter should correspond to an integer value (within the standard error of estimation), and the results of the calculations support this hypothesis. Application of the generalized PU methodology allows for a significant extension of the U_2 class of PU discovered by [6]—it originally contained only subclass U_2^0 represented by the WBE and von Bertalanffy growth functions. Improvement of the original CDG approach to include the generating function (3) allowed us to obtain [11] the following new subclasses: U_2^1, embracing the universal growth curve [5], and U_2^2, for the self-similar fractal function [12]. The results obtained here enriches the U_2 class by U_2^3 represented by the sigmoid and involuted Richards growth models in the hyperbolic representation unknown so far in the area of biosciences and beyond. This model cannot be derived in the original CDG approach [6], where the parameter c_0, relevant for derivation, is neglected. The hyperbolic solution of the CDG equations can be employed to solve the Fokker–Planck equation [10] and generate the time-dependent probability distribution function. This framework can be further generalized through the incorporation of stochastic differential equations (SDEs) [37–39], wherein the growth equation is augmented by a perturbative term that accounts for stochastic (e.g., Brownian or Wiener) processes. This stochastic component introduces a statistical influence factor that enhances the realism of the growth functions by modifying the deterministic growth trajectories reproduced by conventional models.

Funding: This research received no external funding.

Data Availability Statement: The data reported can be found in the papers specified in the references.

Conflicts of Interest: The author declares no conflicts of interest.

Abbreviations

The following abbreviations are used in this manuscript:

AIC	Akaike Information Criterion
BIC	Bayesian Information Criterion
CDG	Castorina Delsanto Guiot
NSD	Normalized Standard Deviation
PU	Phenomenological Universalities
PU-SIR	Phenomenological Universalities Susceptible–Infective–Removed
SD	Standard Deviation
SDE	Stochastic Differential Equation
SIR	Susceptible–Infective–Removed

References

1. Gilbert, S.F. *Developmental Biology*; Sinauer Associates: Sunderland, MA, USA; Swarthmore College: Swarthmore, PA, USA, 2000; ISBN 10:0-87893-243-7.
2. Bertalanffy, V.L. Problems of organic growth. *Nature* **1949**, *163*, 156–158. [CrossRef] [PubMed]
3. Bertalanffy, V.L. Quantitative laws in metabolism and growth. *Q. Rev. Biol.* **1957**, *32*, 217–231. [CrossRef]
4. Richards, F.J. A flexible growth function for empirical use. *J. Exp. Bot.* **1959**, *10*, 290–300. [CrossRef]
5. West, G.B.; Brown, J.H.; Enquist, B.J. A general model for ontogenetic growth. *Nature* **2001**, *413*, 628–631. [CrossRef]
6. Castorina, P.; Delsanto, P.P.; Guiot, C. Classification Scheme for Phenomenological Universalities in Growth Problems in Physics and Other Sciences. *Phys. Rev. Lett.* **2006**, *96*, 188701. [CrossRef]
7. Gliozzi, A.S.; Guiot, C.; Delsanto, P.P. A new computational tool for the phenomenological analysis of multipassage tumor growth curves. *PLoS ONE* **2009**, *4*, e5358. [CrossRef]

8. Barberis, L.; Condat, C.A.; Gliozzi, A.S.; Delsanto, P.P. Concurrent growth of phenotypic features: A phenomenological universalities approach. *J. Theor. Biol.* **2010**, *264*, 123–129. [CrossRef]
9. Barberis, L.; Condat, C.A. Describing interactive growth using vector universalities. *Ecol. Model.* **2012**, *227*, 56–63. [CrossRef]
10. Molski, M. Extended class of phenomenological universalities. *Phys. Lett.* A **2017**, *381*, 2629–2635. [CrossRef]
11. Molski, M. Quantum and classical phenomenological universalities. *Phys. Lett.* A **2018**, *382*, 79–84. [CrossRef]
12. Golmankhaneh, A.K.; Tunç, S.; Schlichtinger, A.M.; Asanza, D.M.; Golmankhaneh, A.K. Modeling tumor growth using fractal calculus: Insights into tumor dynamics. *Biosystems* **2024**, *235*, 105071. [CrossRef] [PubMed]
13. Tjørve, E.; Tjørve, K.M.C. A unified approach to the Richards model family for use in growth analysis: Why we need only two model forms. *J. Theor. Biol.* **2010**, *267*, 417–425. [CrossRef] [PubMed]
14. Molski, M. Theoretical modeling of pre and postnatal growth. *J. Theor. Biol.* **2018**, *458*, 58–67. [CrossRef] [PubMed]
15. Laird, A.K. Dynamics of tumor growth. *Br. J. Cancer* **1964**, *18*, 490–502. [CrossRef] [PubMed Central]
16. Akaike, H. A new look at the statistical model identification. *IEEE Trans. Autom. Control* **1974**, *19*, 716–723. [CrossRef]
17. Schwarz, G. Estimating the dimension of a model. *Ann. Stat.* **1978**, *6*, 461–464. [CrossRef]
18. Myhrvold, N.P. Revisiting the estimation of dinosaur growth rates. *PLoS ONE* **2013**, *8*, e81917. [CrossRef]
19. Rhouma, K.B.; Sakly, M. Involution of rat thymus: Characterization of cytoplasmic glucocorticoid receptors, evidence of glucocorticoid resistant dexamethasone receptor-positive cells. *Arch. Int. Physiol. Biochim. Biophys.* **1994**, *102*, 97–102. [CrossRef]
20. He, M.; Liang, X.; Wang, K.; Pu, H.; Hu, Y.; Ye, G.; Li, X.; Liu, L. Age-related development and histomorphological observation of bursa of Fabricius in yellow quails. *Can. J. Anim. Sci.* **2015**, *95*, 487–491. [CrossRef]
21. Dampin, N.; Tarnchalanukit, W.; Chunkao, K.; Maleewong, M. Fish growth model for Nile Tilapia (*Oreochromis niloticus*). *Procedia Environ. Sci.* **2012**, *13*, 513–524. [CrossRef]
22. Aggrey, S.E. Comparison of three nonlinear and spline regression models for describing chicken growth curves. *Poult. Sci.* **2002**, *81*, 1782–1788. [CrossRef] [PubMed]
23. Smuts, G.L. Pre- and post-natal growth phenoena of Burchell's zebra Equus burchelli antiquorum. *Koedoe* **1975**, *18*, 69–102. [CrossRef]
24. Kempes, C.P.; Dutkiewicz, S.; Follows, M.J. Growth, metabolic partitioning, and the size of microorganisms. *Proc. Natl. Acad. Sci. USA* **2012**, *109*, 495–500. [CrossRef] [PubMed]
25. Sugiura, K.; Benedict, S.R. The influence of certain diets upon tumor susceptibility and growth in albino rats. *J. Cancer Res.* **1920**, *5*, 373–401.
26. Lee, S.A. Incubation times of dinosaur eggs via embryonic metabolism. *Phys. Rev. E* **2016**, *94*, 022402. [CrossRef]
27. Hethcote, H.W. The Mathematics of Infectious Diseases. *SIAM Rev.* **2000**, *42*, 599–653. [CrossRef]
28. Kröger, M.; Schlickeiser, R. Analytical solution of the SIR-model for the temporal evolution of epidemics. Part A: Time-independent reproduction factor. *J. Phys. Math. Theor.* **2020**, *53*, 505601. [CrossRef]
29. Schlickeiser, R.; Kröger, M. Analytical solution of the SIR-model for the temporal evolution of epidemics. Part B: Semi-time case. *J. Phys. Math. Theor.* **2021**, *54*, 175601. [CrossRef]
30. Sivaraman, N.K.; Gaur, M.; Baijal, S.; Muthiah, S.B.; Sheth, A. Exo-SIR: An epidemiological model to analyze the impact of exogenous spread of infection. *Int. J. Data Sci. Anal.* **2025**, *19*, 303–318. [CrossRef]
31. Wanga, X.-S.; Wu, J.; Yang, Y. Richards model revisited: Validation by and application to infection dynamics. *J. Theor. Biol.* **2012**, *313*, 12–19. [CrossRef]
32. van den Driessche, P. Reproduction numbers of infectious disease models. *Infect. Dis. Model.* **2017**, *2*, 288–303. [CrossRef]
33. Biazae, J. Solution of the epidemic model by Adomian decomposition method. *Appl. Math. Comput.* **2006**, *173*, 1101–1106. [CrossRef]
34. Rafei, H.; Daniali, H.; Ganji, D.D. Variational iteration method for solving the epidemic model and the prey and predator problem. *Appl. Math. Comput.* **2007**, *186*, 1701–1709. [CrossRef]
35. Rafei, H.; Ganji, D.D.; Daniali, H. Solution of the epidemic model by homotopy perturbation method. *Appl. Math. Comput.* **2007**, *187*, 1056–1062. [CrossRef]
36. Engida, H.A.; Theuri, D.M.; Gathungu, D.; Gachohi, J.; Alemneh, H.T. A mathematical model analysis for the transmission dynamics of leptospirosis disease in human and rodent populations. *Comput. Math. Methods Med.* **2022**, *1*, 1806585. [CrossRef] [PubMed]
37. Kapur, P.K.; Anand, S.; Yamada, S.; Yadavalli, V.S.S. Stochastic Differential Equation-Based Flexible Software Reliability Growth Model. *Math. Probl. Eng.* **2009**, *2009*, 581383. [CrossRef]

38. Samoletov, A.; Vasiev, B. A mathematical framework for the statistical interpretation of biological growth models. *BioSystems* **2024**, *246*, 105342. [CrossRef]
39. Baltazar-Larios, F.; Delgado-Vences, F.; Ornelas, A. Parameter estimation and model selection for stochastic differential equations for biological growth. *Environ. Ecol. Stat.* **2025**, *32*, 195–227. [CrossRef]

Disclaimer/Publisher's Note: The statements, opinions and data contained in all publications are solely those of the individual author(s) and contributor(s) and not of MDPI and/or the editor(s). MDPI and/or the editor(s) disclaim responsibility for any injury to people or property resulting from any ideas, methods, instructions or products referred to in the content.